

A New Approach to Statistics of Cosmological Gamma-Ray Bursts

M. Böttcher^{1,2} & C. D. Dermer²

Submitted to the Astrophysical Journal

ABSTRACT

We use a new method of analysis to determine parameters of cosmological gamma-ray bursts (GRBs), assuming that their distribution follows the star-formation history of the universe. Spectral evolution is calculated from an external shock model for fireball/blast wave evolution, and used to evaluate the measured peak flux, duration, and νF_ν peak photon energy for a GRB source occurring at a given redshift and with given values of total energy, baryon-loading and environmental parameters. We then fit model distributions of GRB sources to the observed peak flux, duration and νF_ν peak photon energy distributions. We find that the observed width of the E_p and duration distributions can not be explained by cosmological redshift and time dilation effects. Rather, broad distributions of total blastwave energies and bulk Lorentz factors are necessary to explain the observed distributions simultaneously within the framework of our unifying GRB model. We discuss implications for source parameter distributions and determine a range of burst parameters consistent with the data.

Subject headings: cosmology: theory — gamma-rays: bursts — gamma-rays: theory — radiation mechanisms: non-thermal

1. Introduction

The extragalactic origin of GRBs has been confirmed with the discovery of X-ray, optical and radio afterglows of GRBs as a result of the Italian-Dutch Beppo-SAX mission (e.g., Costa et al. 1997; van Paradijs et al. 1997; Frail 1998). At present, there are 8 GRBs with redshifts obtained from emission line measurements of host galaxy counterparts. These are GRB 980425 at redshift $z = 0.0084$ (Kulkarni et al. 1998a), GRB 970228 at $z = 0.695$ (Djorgovski et al.

¹Rice University, Space Physics and Astronomy Department, MS 108
6100 S. Main Street, Houston, TX 77005 – 1892, USA

²E. O. Hulburt Center for Space Research, Code 7653,
Naval Research Laboratory, Washington, D. C. 20375-5352

1999a), GRB 970508 at $z = 0.835$ (Bloom et al. 1998a), GRB 970828 at $z = 0.958$ (Djorgovski 1999), GRB 980703 at $z = 0.966$ (Djorgovski et al. 1998), GRB 980613 at $z = 1.096$ (Djorgovski et al. 1999b), GRB 990123 at $z = 1.60$ (Kelson et al. 1999) and GRB 971214 at $z = 3.418$ (Kulkarni et al. 1998b). The redshift inferred for GRB 980425 depends on the validity of the GRB 980425/SN1998bw association (Galama et al. 1998). The host galaxy redshift of GRB 970508 supports the original redshift report obtained through absorption line measurements in its fading optical counterpart (Metzger et al. 1997), and is strengthened by the recent Beppo-SAX announcement (Piro et al. 1999) of a redshifted iron fluorescence feature found in the spectrum of its fading X-ray counterpart between $\approx 2.5 \times 10^4$ and 6×10^4 s following GRB 970508.

It is not possible to construct a reliable GRB redshift distribution from the statistics of eight GRBs. Except for GRB 980425, however, whose nature remains controversial, the obtained redshifts place most GRBs at the cosmological epoch of active star formation. Several models for the origin of GRBs, such as the collapsar/hypernova scenario (Woosley 1993; Paczyński 1998) or the supranova scenario of Vietri & Stella (1998), suggest that GRBs are physically related to recent star formation. Their cosmological distribution should therefore trace the star formation history of the universe (Totani 1997). An origin of GRBs involving stellar collapse events is also in accord with the small measured offsets of fading transient GRB counterparts with respect to the disks of the candidate host galaxies (Kulkarni 1998, Bloom et al. 1999). By contrast, a larger offset is expected in the compact object coalescence scenario (e.g., Eichler et al. 1989; Narayan, Paczyński, & Piran 1992) and, moreover, the redshift distribution of GRBs in this scenario is not required to follow the star formation history of the universe due to the large time delays between the formation and merging of compact object binaries.

Several authors have calculated the GRB peak flux distribution, testing the assumption of a GRB rate proportional to the observed star formation rate as given, e. g., by Lilly et al. (1996) and Madau et al. (1996). Krumholz et al. (1998) demonstrated that besides a GRB spatial distribution following the star formation rate of the universe, a variety of other luminosity and redshift distributions of cosmological GRBs are consistent with the observed peak flux distribution. Totani (1999) used an empirical correlation between the observed time-integrated spectral shape of GRBs and their peak flux, and finds that the resulting peak flux distribution is only consistent with the star formation history of the universe if the star formation rate between $z = 0$ and 1 is much flatter ($SFR[z = 1] \sim 4 \times SFR[z = 0]$) than deduced from UV observations ($SFR[z = 1] \sim 15 \times SFR[z = 0]$), the former evolution being in agreement with independent estimates on the basis of galaxy evolution models (Totani et al. 1997). He finds similar results for models invoking binary neutron star or neutron star – black-hole mergers. In contrast, Wijers et al. (1998), assuming a standard-candle luminosity of GRBs, find reasonable agreement between their theoretical peak flux distribution and the one deduced from BATSE/PVO observations.

This controversy indicates that the peak flux distribution data alone do not sufficiently constrain GRB parameters, in particular their luminosity and redshift distributions. Recently, Kommers et al. (1998) have included very faint, “non-triggered” BATSE GRBs in a peak

flux distribution study and demonstrated that even this improved data set cannot confidently distinguish between a GRB rate tracing the star formation rate and one tracing the redshift distribution of AGNs.

Previous theoretical GRB peak flux distribution studies have either used simple, non-evolving representations of the intrinsic burst spectra, such as a thermal bremsstrahlung spectrum (Fenimore et al. 1993) or a single power-law (Krumholz et al. 1998), or have summed over a sample of observed, time-integrated spectra (Fenimore & Bloom 1995, Wijers et al. 1998, Kommers et al. 1998). Mallozzi et al. (1996) demonstrated that the assumed intrinsic spectral shape of GRBs has a significant influence on the results of theoretical GRB peak flux distribution studies.

The first attempt to combine peak flux distribution studies with other statistical properties was done by Fenimore & Bloom (1995), who deduced a typical distance scale for GRBs from the observed effect of time dilation on the burst duration by comparing the brightest and dimmest BATSE bursts. They found that in order to explain a time dilation by a factor of 2, the dimmest bursts had to be located at $z > 6$. However, they pointed out that the implied isotropic burst luminosity was inconsistent with the observed peak flux distribution, even in the case of a strong cosmological evolution of the comoving burst rate and of the luminosity if both evolutions are parametrized as power-laws in $(1 + z)$. However, the significance of the observed peak flux – duration correlation is highly controversial. Mitrofanov et al. (1993) did not find any evidence for time dilation between dim and bright bursts, while Norris et al. (1994) deduced a maximum redshift of $z \sim 2.25$ for the dimmest bursts from time dilation effects.

Here we demonstrate the importance of considering additional statistical properties to constrain the intrinsic and environmental properties of GRB fireballs. These include the duration distribution and the distribution of peak energies E_p of the time-averaged νF_ν spectra of GRBs. The duration distribution of BATSE GRBs shows a pronounced bimodality (Kouveliotou et al. 1993) between short ($t_{50} \lesssim 0.5$ s) and long ($t_{50} \gtrsim 3$ s) bursts. This has been interpreted as evidence for two physically distinct source populations by Katz & Canel (1996), who found that the $\langle V/V_{max} \rangle$ distribution of the populations of short and long bursts are significantly different from each other. Both populations show evidence for a cosmological origin ($\langle V/V_{max} \rangle < 0.5$), but the long bursts with $\langle V/V_{max} \rangle = 0.282 \pm 0.014$ are located at larger distances and/or exhibit stronger cosmological evolution than the short bursts with $\langle V/V_{max} \rangle = 0.385 \pm 0.019$. This was confirmed by Tavani (1998) who found that the long / hard bursts show significantly stronger deviations from a uniform distribution in Euclidean space than other subclasses of GRBs.

The νF_ν peak energies E_p vary from burst to burst, although most are between ≈ 50 keV and 1 MeV (Mallozzi et al. 1997; Strohmayer et al. 1998). Assuming that the range of E_p intrinsic to the burst sources does not evolve with redshift, Mallozzi et al. (1995) found that the E_p vs. peak flux distribution of BATSE bursts indicates a maximum redshift range of $(1 + z_1)/(1 + z_{100}) = 1.86_{-0.24}^{+0.36}$ between bursts with peak fluxes of 1 and 100 photons $\text{cm}^{-2} \text{s}^{-1}$, respectively.

Previous work on modeling the peak flux distribution of cosmological GRBs has mainly been carried out in a model-independent way, using phenomenological representations of the burst spectral and temporal properties, without specifying physical parameters of the burst sources. In particular, detailed predictions of theoretical blast-wave models for the peak power and temporal evolution of GRB spectra have never been used to model the observed statistics of GRBs. In this paper, we use a parametric description of the spectrum and spectral evolution predicted by the external shock model for cosmological GRBs (Dermer et al. 1999a) to calculate self-consistently the peak flux of a GRB at a given redshift, its duration t_{50} , and the observed peak energy E_p of the νF_ν spectrum. Assuming that GRBs trace the star formation history of the universe, this analysis helps to constrain not only the total energy of GRBs, but additional parameters such as the initial Lorentz factor (or baryon loading factor) Γ_0 of the GRB blast wave, the total energy E_0 deposited into the blast wave, the density of the circumburst material (CBM), and the equipartition factor q , which parametrizes the magnetic field strength and efficiency of electron acceleration in the blast wave.

In Section 2, we present the model equations for a GRB from a fireball/blast wave which is energized, decelerates, and radiates by its interaction with a smooth CBM. We apply BATSE triggering criteria to this model in order to extract measured values of peak flux, duration and peak energy. A function describing the star formation history of the universe is given. In Section 3, we calculate peak flux, t_{50} , and E_p distributions for a GRB source population involving ranges of baryon loading factors and total fireball energies. Fits to the observed distributions are presented. The results are discussed in Section 4, and we summarize with implications for source models of GRBs.

2. Peak Fluxes, Peak Energies, and Burst Durations

Following the treatment given by Dermer et al. (1999a), the photon number spectrum from a GRB located at redshift z and its temporal evolution is parametrized by the expression

$$\Phi(\epsilon, t; z) = \frac{1}{4\pi d_L^2 \epsilon^2 m_e c^2} \frac{(1 + \frac{\nu}{\delta}) P_p(t)}{[\epsilon/\epsilon_p(t)]^{-\nu} + (\nu/\delta) [\epsilon/\epsilon_p(t)]^\delta}, \quad (1)$$

where $\epsilon = E/(m_e c^2)$ is the dimensionless photon energy, d_L is the luminosity distance to the burst, ν and δ are the asymptotic low-energy and high-energy νF_ν slopes of the GRB spectrum, and t is the time in the observer's frame. Throughout this study we use $\nu = 4/3$, while a distribution of high-energy slopes $N(\delta) \propto \delta^{-0.5}$ for $\delta \geq 0.05$ is assumed (obviously, the normalization of the spectral representation [1] diverges for $\delta \leq 0$). This distribution is in reasonable agreement with the distribution of GRB spectral indices with photon number indices > 2 determined in the statistical analysis of high-energy spectra of BATSE GRBs by Preece et al. (1998a). The measured distribution is only an approximation to the asymptotic high-energy distribution of slopes because the BATSE sensitivity range does not always sample photons with energies $\epsilon \gg \epsilon_p$.

The νF_ν peak photon energy is given by

$$\epsilon_p(t) = 3.0 \cdot 10^{-8} \frac{qn_0^{1/2}\Gamma_0^4}{1+z} \begin{cases} x^{-\eta/2} & \text{for } 0 \leq x < 1 \\ x^{-4g-\eta/2} & \text{for } 1 \leq x \leq \Gamma_0^{1/g}. \end{cases} \quad (2)$$

Here, $q = \sqrt{\xi_H(r/4)} \xi_e^2$ is the combined equipartition factor, containing the magnetic field equipartition factor ξ_H , the electron equipartition factor ξ_e , and the shock compression ratio r , and Γ_0 is the initial bulk Lorentz factor or baryon loading factor of the blast wave. The term η is the power-law index of the surrounding CBM density structure, given by the smoothly varying function

$$n(x) = n_0 x^{-\eta}. \quad (3)$$

The CBM is assumed to be isotropically distributed about the source of the GRB. For simplicity, we let $\eta = 0$ in the calculations presented here. The term $x = R/R_d$ is the radial coordinate R in units of the deceleration radius R_d , and is related to the observing time t by

$$x = \begin{cases} \frac{t}{t_d} & \text{for } 0 \leq x \leq 1 \\ \left[(2g+1) \frac{t}{t_d} - 2g \right]^{1/(2g+1)} & \text{for } 1 \leq x \leq \Gamma_0^{1/g}. \end{cases} \quad (4)$$

Here t_d is the deceleration time scale of the blast wave in the observer's frame, given by

$$t_d = \frac{1+z}{c\Gamma_0^{8/3}} \left[\frac{(3-\eta)E_0}{4\pi n_0 m_p c^2} \right]^{1/3}, \quad (5)$$

and g parametrizes the radiative regime. For a non-radiative (adiabatic) blast wave, $g = 3/2 - \eta$, while $g = 3 - \eta$ describes a fully radiative blast wave. Throughout this study, we assume that the blast wave is uncollimated. Beaming can be approximately implemented in the prompt and early afterglow phases of a GRB by replacing the total energy E_0 with the quantity $4\pi(\partial E_0/\partial\Omega)$, where $\partial E_0/\partial\Omega$ is the energy radiated per steradian into the solid angle element whose normal is directed within an angle $\lesssim 1/\Gamma_0$ of the direction to the observer. The peak νL_ν luminosity $P_p(t)$ depends on the parameters of the model according to the relation

$$P_p(t) = \frac{c(2g-3+\eta)(4\pi m_p c^2)^{1/3}}{2g(v^{-1}+\delta^{-1})(1+z)^2} n_0^{1/3} E_0^{2/3} \Gamma_0^{8/3} \begin{cases} x^{2-\eta} & \text{for } 0 \leq x < 1 \\ x^{2-\eta-4g} & \text{for } 1 \leq x \leq \Gamma_0^{1/g}. \end{cases} \quad (6)$$

Using Eq. (1), we determine the peak flux $\Phi_p(z)$ of a GRB, averaged over the BATSE trigger time scale Δt in the 50 - 300 keV energy range, by scanning through t_1 and finding the maximum of the expression

$$\Phi_p(z) = \max_{t_1} \left\{ \frac{1}{\Delta t} \int_{t_1}^{t_1+\Delta t} dt \int_{\epsilon_1}^{\epsilon_2} d\epsilon \Phi(\epsilon, t; z) \right\}, \quad (7)$$

where $\epsilon_1 = 50/511$ and $\epsilon_2 = 300/511$. A burst producing a peak flux Φ has a probability $P_{\text{tr}}(\Phi)$ to trigger BATSE. We parametrize the trigger efficiencies given by Fishman et al. (1994) by

$$P_{\text{tr}}(\Phi) = \exp[-(\Phi_0/\Phi)^\alpha], \quad (8)$$

where Φ_0 and α depend on the trigger time scale:

$$\begin{aligned}\Phi_{0,1024} &= 0.26 \text{ photons cm}^{-2} \text{ s}^{-1}, & \alpha_{1024} &= 5.3 \\ \Phi_{0,256} &= 0.53 \text{ photons cm}^{-2} \text{ s}^{-1}, & \alpha_{256} &= 5.7 \\ \Phi_{0,64} &= 1.05 \text{ photons cm}^{-2} \text{ s}^{-1}, & \alpha_{64} &= 5.5\end{aligned}\tag{9}$$

The different effective trigger thresholds are mainly due to effects of variable background. In addition, the trigger criterion corresponding to $\Delta t = 1024$ ms involves a selection bias toward bursts with durations $\gtrsim 1$ s. Due to this duration bias, shorter bursts with the same peak flux are less likely to trigger a GRB telescope because the total number of detected photons during the trigger time scale is smaller. Thus the effective integration time is determined in this case by the burst duration rather than the trigger time scale.

For a given peak flux value Φ_p and a given set of GRB parameters, an approximate limiting redshift $z_{\max}(\Phi_p)$ can be defined at which the GRB produces a peak flux $\Phi_p(z_{\max}) = \Phi_0$ corresponding to the respective trigger time scale. Fig. 1 illustrates how z_{\max} of a standard GRB varies with Γ_0 , q , and δ for the 1024 ms trigger criterion. For fixed values of q , the peak flux increases with increasing Γ_0 until E_p attains values greater than the photon energies of the detector triggering range. At larger values of Γ_0 , the emission recorded by a detector is dominated by the synchrotron emissivity spectrum $F_\nu \propto \nu^{1/3}$ produced by a distribution of electrons with a low-energy cutoff. Because this portion of the spectrum is so hard, the peak flux, and therefore z_{\max} , declines at larger values of Γ_0 , as shown in Fig. 1.

The Lorentz factor $\bar{\Gamma}_0$ of a fireball which produces the maximum peak flux in a detector sensitive to photons with energy E_d is given by $\bar{\Gamma}_0 \approx 75 [(1+z)E_d/(m_e c^2 q n_0^{1/2})]^{1/4}$, using eq. (2). The nominal BATSE triggering range, as noted above, is $50 \text{ keV} \leq E_d \leq 300 \text{ keV}$. For values of $\Gamma_0 \gtrsim \bar{\Gamma}_0$, z_{\max} is anticorrelated with q because for larger q the νF_ν peak is shifted towards higher frequencies, causing the (Γ_0, z_{\max}) curves to level off at lower values of Γ_0 . The maximum redshift is also very sensitive to changes in δ for $\Gamma_0 \gtrsim \bar{\Gamma}_0$. This is a consequence of the fact that a rapidly increasing fraction of the radiated energy is emitted at $E > 300$ keV as δ approaches 0. Obviously, z_{\max} is also strongly dependent on the radiative regime g , determining the fraction of the available energy which is converted into radiation.

A differential peak flux distribution is calculated from the relation

$$\Delta \dot{N}(\Phi_i < \Phi_p < \Phi_{i+1}) = \frac{4\pi c}{H_0} \int_{z_{\max}(\Phi_{i+1})}^{z_{\max}(\Phi_i)} dz \frac{\dot{n}_{GRB}(z) d_L^2 P_{\text{tr}}(\Phi_p[z])}{(1+z)^3 \sqrt{(1+\Omega_0 z)(1+z)^2 - \Omega_\Lambda (2z+z^2)}}, \tag{10}$$

(Totani 1999), where we choose $(\Omega_0, \Omega_\Lambda) = (0.3, 0.7)$ and $H_0 = 65 \text{ km s}^{-1} \text{ Mpc}^{-1}$. In this cosmology the luminosity distance d_L is

$$d_L = \frac{c}{H_0} (1+z) \int_0^z \frac{dz'}{\sqrt{(1+\Omega_0 z')(1+z')^2 - \Omega_\Lambda (2z'+z'^2)}}. \tag{11}$$

Note that Eq. (10) refers to a mono-parametric distribution of burst sources, for which a unique relation between peak flux and redshift holds. In the lowest flux bin ($\Phi_0 < \Phi_p < \Phi_1$), the number of detected bursts will be determined by the trigger probability. Consequently, we use $z_{max}(\Phi_0) = \infty$. $\dot{n}_{GRB}(z)$ is the comoving burst rate per comoving unit volume. We assume that $\dot{n}_{GRB}(z)$ is proportional to the star formation rate (SFR), for which we use a simple representation of the function shown in Madau et al. (1998):

$$SFR(z)[M_{\odot} \text{ yr}^{-1} \text{ Mpc}^{-3}] = \begin{cases} 10^{-3} \cdot 10^{z+1} & \text{for } z \leq 1.1 \\ 0.13 & \text{for } 1.1 < z \leq 2.8 \\ 4.2 \cdot 10^{-0.4(z+1)} & \text{for } z > 2.8. \end{cases} \quad (12)$$

The νF_{ν} peak energy of the burst spectrum as a function of redshift is evaluated at the time $t = t_d$ of peak power output of the GRB using eq. (2). Thus $E_p/(m_e c^2) = 3.0 \times 10^{-8} q n_0^{1/2} \Gamma_0^4 / (1 + z)$.

For the duration distribution, we calculate t_{50} as the duration between the times when 25% and 75% of the total photon fluence in the 50 – 300 keV band (from eq. [1]) has been received. In Fig. 2 we plot t_{50} as a function of Γ_0 , q , and δ for a standard GRB located at $z = 1$. For small values of Γ_0 , for which E_p is below or within the detector energy range, t_{50} is proportional to the deceleration time $t_d \propto \Gamma_0^{-8/3}$. For larger Γ_0 , E_p is above the detector energy range, and the burst duration is determined by the time it takes for the νF_{ν} peak of the evolving burst spectrum to sweep through the detector energy range. For the parameters assumed here, t_{50} is only weakly dependent on the initial bulk Lorentz factor in the high- Γ_0 limit. Using the asymptotic forms of eq. (1) and realizing that most photons are produced after $E_p(t)$ has swept through the detector energy range, one can analytically show that $t_{50} \propto t_d \Gamma_0^{(2g+1)/(g+\eta/8)} \propto \Gamma_0^{(1/g)-(2/3)}$ if $\Gamma_0 \gg \bar{\Gamma}_0$, where the last expression holds when $\eta = 0$.

The burst duration t_{50} is independent of the equipartition parameter q for small values of Γ_0 and weakly positively correlated with q for high Γ_0 . There is a very strong correlation between the burst duration and the high-energy spectral index. As δ approaches 0, t_{50} increases drastically since the very hard tail of the spectrum produces a “ γ -ray afterglow” which decays with time $\propto t^{-\chi}$, where $\chi = [4g(1 + \delta) - 2]/[2g + 1]$ for $\eta = 0$. This approaches a t^{-1} decay if $\delta \rightarrow 0$ and $g \approx 1.5$. The duration is also correlated with the radiative regime g with t_{50} decreasing by an approximately constant factor over the entire Γ_0 range considered here as g increases. For typical parameters, this downward shift can reach a factor of ~ 10 as g spans the range from 1.5 to 3.

The E_p and t_{50} distributions are calculated simultaneously while scanning through redshift space according to Eq. (10). We caution that our analysis does not take into account any effects due to the instrumental noise or the diffuse radiation backgrounds recorded by the BATSE detectors. The actual t_{50} and t_{90} durations of a GRB are expected to be slightly longer than measured because the additional background noise will dominate the emissions from a GRB at early and late times, particularly for weak GRBs. The actual E_p distribution of those GRBs which trigger BATSE is, however, not expected to be much different from the measured E_p distribution, because the background spectrum is subtracted in the spectral analyses which yield E_p (see, e.g., Mallozzi et al. 1995).

3. Comparison with Observed Distributions

We first applied the formalism described in the previous section to calculate peak flux, E_p , and duration distributions from cosmological GRBs with a single set of values for the burst parameters. The theoretical distributions were compared with the peak flux and duration distributions from the Third BATSE GRB catalog as compiled by Meegan et al. (1996), and to the E_p distribution of Mallozzi et al. (1997). The values of E_p were evaluated by Mallozzi et al. (1997) by fitting the GRB spectrum from the 4B catalog (Meegan et al. 1997) with the Band function (Band et al. 1993). We use the trigger time scale $\Delta t = 1024$ ms, corresponding to a peak flux threshold of $\Phi_{trig} \approx 0.2$ photons $\text{cm}^{-2} \text{s}^{-1}$. This is the trigger criterion used to extract the peak flux distribution data shown in Meegan et al. (1996) and in our Figs. 3, 4, and 5. We note that our analysis is properly applied to data sets which are produced by uniform triggering criteria, but that the E_p distribution might be biased with respect to the duration and peak flux distributions since the E_p data can be obtained only for the brighter GRBs. Moreover, the E_p analysis uses 16 energy channel data, whereas the peak fluxes are based on the four energy channel discriminator data (R. Mallozzi, private communication, 1998). A uniform selection criterion for the peak flux, duration and E_p distributions should be considered in future studies.

Figs. 3 and 4 show the derived distributions of GRB sources for mono-parametric models of the blast wave and surrounding medium. The spread of measured values is thus a consequence of distance and cosmological effects and the GRB rate history, assumed throughout this paper to be proportional to the star formation rate SFR (Eq. [12]). The dependence of the observables on the radiative index g which parametrizes the radiative regime and thus determines the luminosity of the GRB, are shown in the individual figures. While the redshift and thus the peak flux distributions are very sensitive to slight changes in g , the E_p and t_{50} distributions are rather insensitive to the radiative regime. A comparison of Fig. 3 and 4 demonstrates the sensitivity of the resulting distributions on the total energy $E_0 = 10^{52} E_{52}$ erg. The figures also show that the spread in E_p and t_{50} due to cosmological redshift alone is far less than the width of the observed distributions, indicating that they are probably dominated by a spread in the intrinsic GRB properties.

We note that our modeling result is not unique. There is at least one ambiguity in the sense that virtually indistinguishable peak flux, E_p and duration distributions are obtained when varying the CBM density n_0 and the initial bulk Lorentz factor Γ_0 , keeping the product $n_0 \Gamma_0^8$ constant. The reason for this ambiguity lies in the fact that the peak flux, E_p , and t_d all depend only on the product $n_0 \Gamma_0^8$ (see eqs. [7], [2], and [5]). An average density of $n_0 \sim 10^2 - 10^5 \text{ cm}^{-3}$ seems to be appropriate if GRBs are correlated with star-forming regions.

As can be seen, the peak flux, duration, and E_p distributions measured with BATSE requires fireballs with energies $\sim 10^{52} - 10^{53}$ ergs, baryon-loading factors corresponding to $\Gamma_0 \sim 200 - 300$, and an equipartition factor $q \sim 10^{-3}$. The mean redshifts of such GRB sources lie typically near $z \sim 1$. The ability of the external shock model to account for the characteristic duration of GRBs

was first noted by Rees and Mészáros (1992).

Fig. 5 shows the results of evaluating a large set ($N \sim 2000$) of mono-parametric burst distributions and subsequently adding these distributions according to a variety of intrinsic parameter distributions. Apart from the high-energy slopes δ (see previous section), the total fireball energy E_{52} and the bulk Lorentz factor Γ_0 , are assumed to be distributed according to truncated power-laws, $N(E_{52}) \propto E_{52}^{-e}$, $N(\Gamma_0) \propto \Gamma_0^{-\gamma}$. The power-law indices e and γ , and the boundaries $\Gamma_{0,\min}$, $\Gamma_{0,\max}$ are free parameters. Comparing the lower limits on E_{52} deduced from observations of different GRBs, such as GRB 970508 (e.g., Waxman 1997), GRB 980703 (Bloom et al. 1998b), and GRB 971214 (Kulkarni et al. 1998b), not to mention GRB 980425 (Kulkarni et al. 1998a), we know that the total available energy in the blast wave may well vary from source to source by several orders of magnitude. We assume that the values of E_{52} vary in the range $E_{52,\min} = 10^{-4}$ and $E_{52,\max} = 100$. We find that the resulting peak flux, E_p , and t_{50} distributions are only weakly dependent on the actual values of these boundaries. Bursts with $E_{52} \lesssim 10^{-3}$ are only detectable at very small redshifts where the number density of burst sources is assumed to be small due to the strong evolution of the star-formation rate (see eq. [12]). They thus contribute very little to the observed distributions. For power-law indices $e \gtrsim 1$, the number of bursts with $E_{52} \gtrsim 100$ is strongly reduced compared to the lower-energy bursts, so that the contribution of bursts with energies beyond this value is of minor importance as well.

Dermer et al. (1999a, 1999b) argue that there could be a wide distribution in the baryon loading factor of GRB fireballs, of which preferentially those sources with νF_ν peaks between ~ 50 keV – several MeV, corresponding to a baryon loading factor of $\Gamma_0 \approx \bar{\Gamma}_0$, are detected due to the triggering criteria of currently operating GRB monitors and the limitations of telescopes at X-ray and \gg MeV energies. Detectability of burst sources with values of $\Gamma_0 \ll \bar{\Gamma}_0$ is strongly reduced because most of the flux will be emitted at energies below the sensitivity threshold of BATSE. The same is true, though to a lesser extent, for fireballs which produce blast waves with $\Gamma_0 \gg \bar{\Gamma}_0$. Thus we expect that the peak flux distribution observed from a population of burst sources with a variety of Γ_0 values will not strongly depend on the actual range of baryon loading factors. However, due to the strong dependence of the peak energy E_p on Γ_0 through eq. (2), we expect that the observed E_p distribution may well be influenced by the shape of the Γ_0 distribution. The dependence of the burst duration on Γ_0 is weaker (see Fig. 2), but still considerable. In terms of the deceleration time t_d , we have $t_d \propto \Gamma_0^{-8/3}$, so that a range in Γ_0 will also lead to a broadening of the t_{50} distribution for a fixed value of n_0 .

A reasonable match of our theoretical distributions simultaneously with the peak flux, the E_p and the t_{50} distributions was achieved for $\Gamma_{0,\max} = 260$, $n_0 = 100 \text{ cm}^{-3}$, $g = 1.7$, and $q = 10^{-3}$, $e \sim 1.5$, and $\gamma \sim 0$. A low value of $q \lesssim 10^{-3}$ is in agreement with the results of Chiang & Dermer (1999), who argue that such a small equipartition parameter is required in order to prevent rapid synchrotron cooling. A much larger value of q would result in a low-energy synchrotron spectrum $\Phi(\epsilon) \propto \epsilon^{-3/2}$, inconsistent with the observed hard low-energy asymptotes of BATSE GRB spectra (Band et al. 1993, Crider et al. 1997, Preece et al. 1998b). To constrain the intrinsic distributions

in E_{52} and Γ_0 , we fix n_0 , g , q , and $\Gamma_{0,\max}$ to the values quoted above, and let the power-law indices e and γ vary as free parameters. In our fitting procedure we neglect χ^2 contributions from durations $t_{50} < 0.5$ s and from E_p values of < 100 keV because, as mentioned earlier, bursts with $E_p < 100$ keV tend to be too dim to allow the determination of spectral parameters such as E_p . We obtain a best fit simultaneously to all three distributions for $e = 1.52$ and $\gamma = 0.25$. Fig. 5 shows the peak flux, E_p , t_{50} , and calculated redshift distributions from this burst population. Our fits are rather insensitive to the actual distribution of Γ_0 values in terms of $\Gamma_{0,\min}$ and the index γ of the power-law distribution in Γ_0 . GRBs with $\Gamma_0 \approx 220$ are preferentially detected for the value of $n_0 = 100 \text{ cm}^{-3}$ chosen here, and the contribution of dirtier fireballs to the peak flux, E_p , and t_{50} distribution is almost negligible.

Fig. 6 shows the 1σ and 2σ confidence contours for the power-law indices e and γ of the E_{52} and Γ_0 distributions, respectively, if the remaining relevant parameters are fixed to $g = 1.7$, $q = 10^{-3}$, $n_0 = 100 \text{ cm}^{-3}$, and $\Gamma_{0,\max} = 260$. The figure confirms that the actual shape of the distribution of baryon loading factors is only weakly constrained: A large range of γ values ($-0.2 \lesssim \gamma \lesssim 0.7$) yields acceptable fits to all three distributions. In contrast, the power-law in E_{52} is constrained to a narrow range of indices, $1.49 \lesssim e \lesssim 1.54$.

The normalization of our model peak flux distribution requires $\dot{n}_{\text{GRB}}(z) = 4.43 \cdot 10^{-5} \text{ SFR}/M_{\odot}$, which yields a local GRB rate $\dot{n}_{\text{GRB}}(z = 0) = 443 \text{ GRBs yr}^{-1} \text{ Gpc}^{-3}$. Assuming a local galaxy number density of $4.8 \cdot 10^{-3} \text{ Mpc}^{-3}$ (Wijers et al. 1998), this is equivalent to a local GRB rate of 92 Galactic events per Myr. This rate is a factor of 3700 higher than the result of Wijers et al. (1998). However, we note that the population assumed here contains many undetected bursts for the existence of which, consequently, there is no evidence.

The faintest detectable bursts in our model distributions are located beyond a redshift of $z \gtrsim 4$. The maximum of the redshift distribution is located around $z \lesssim 1$, in good agreement with the redshifts from GRBs measured so far. The small number of these GRBs does not yet allow an independent statistical analysis.

It is clear from Fig. 5 that the bimodality of the burst duration cannot be explained with the continuous burst source population assumed in our model calculations. The t_{50} bimodality is not an instrumental effect, but indicates that GRBs consist of at least 2 separate classes, characterized by different physical parameters. The peak flux distribution of Meegan et al. (1996) was constructed on the basis of the 1024 ms trigger criterion, which misses most of the short bursts. Furthermore, all GRBs for which redshifts could be measured as a consequence of their precise localization by the BeppoSAX satellite, belong to the subclass of long bursts. Thus, there is very limited information on the short bursts so far. Therefore we do not attempt to model this subclass of GRBs in this paper. With new data expected from the upcoming HETE II mission, which might enable us to localize also several short bursts and determine their broadband spectral characteristics and redshifts, a global statistical analysis similar to the one presented here might become possible.

The external shock model qualitatively explains the trend (Tavani 1998) that GRBs with harder spectra have, on average, smaller $\langle V/V_{\max} \rangle$ values. Consider the simplification where fireballs are characterized only by Γ_0 and E_0 . Blast waves with larger values of Γ_0 decelerate and radiate more rapidly and emit the bulk of their radiation at shorter wavelengths. They are therefore more luminous (see Fig. 1), shorter and harder. More energetic GRBs have longer durations (eq. [5]). Tavani’s long/hard class of GRBs therefore corresponds to the class of fireballs with the largest values of Γ_0 and E_0 , and these are the ones that can be detected from the greatest distances and therefore exhibit the strongest non-Euclidean effects. By contrast, the long/soft class of GRBs represents less luminous fireballs with smaller mean values of Γ_0 and E_0 . Only being detectable from relatively nearby sites, these would display smaller cosmological effects on the peak flux distribution. Analogous reasoning would also apply to the short class of GRBs, though the bimodality of this population indicates that other parameters must also be taken into account.

We note that the external synchrotron shock model, as parametrized by eq. (1), specifically applies to the so-called “Fast-Rise, Exponential Decay” FRED-like burst light curves (see Fishman & Meegan 1995; Dermer et al. 1999b). While the overall spectral shape and luminosity (which determines the peak flux and E_p distributions) may be similar for more complicated, spiky light curves — which could arise from the interaction of the blast wave with an inhomogeneous medium (Dermer & Mitman 1999) — the observed durations might be altered by this effect. However, the bimodality of the duration distribution is not reasonably explained by a variety of light curves, and probably indicates a bimodality in parameter space (Katz & Canel 1996, Tavani 1998).

4. Summary and Conclusions

We have used the cosmological blast wave model to fit simultaneously the peak flux, E_p , and t_{50} distributions as observed by BATSE, using an analytical representation of the spectral evolution predicted by the external shock model. The GRB source distribution is assumed to trace the star formation history of the universe. For our standard cosmology ($H_0 = 65 \text{ km s}^{-1} \text{ Mpc}^{-1}$, $\Omega_0 = 0.3$, $\Omega_\Lambda = 0.7$), the peak flux and E_p distributions, and the t_{50} distribution of the population of GRBs with durations $t_{50} \gtrsim 0.5 \text{ s}$ can be modeled with a source population characterized by $N(\Gamma_0) \propto \Gamma_0^{-0.25}$, $\Gamma_0 \leq 260$, $N(E_{52}) \propto E_{52}^{-1.52}$, $10^{-4} \leq E_{52} \leq 100$, $g = 1.7$, and $q = 10^{-3}$, if the density of the circumburster material is assumed as $n_0 = 100 \text{ cm}^{-3}$. Equally good fits can be found for different values of the CBM density, if the product $n_0 \Gamma_0^8$ is held constant. Our results are fairly sensitive to the radiative regime of the blast wave and to the value of the equipartition parameter.

The widths of the observed statistical distributions can not be explained solely by cosmological redshift and time dilation effects, but require a broad distribution of intrinsic parameters, in particular of the total blastwave energy E_{52} and the initial bulk Lorentz factor Γ_0 . Assuming that these parameters are distributed according to single power-laws, the E_{52} distribution is well constrained for a fixed set of parameters which gives a good fit to the distributions, while the

modeling results are rather insensitive to the detailed shape of the Γ_0 distribution.

Our model calculation implies a local GRB rate of 443 GRBs $\text{yr}^{-1} \text{Gpc}^{-3}$ or 92 Galactic events per Myr. This is a higher rate than obtained in some recent estimates (e.g., Wijers et al. 1998) and indicates a better chance of detecting relatively young ($\lesssim 10^4$ yr) GRB remnants in nearby galaxies. The photoionization signatures of such young GRB remnants recently investigated in detail by Perna et al. (1999) might then serve as a critical test for the assumed correlation between GRBs and star-forming regions.

The bimodality of the t_{50} distribution can only be explained in the context of the present model if a bimodality in GRB source parameter space is assumed.

The simplified analytic form used to represent the observed spectra from cosmological blast waves provides a reasonable representation of all three statistical distributions considered in this paper, thus lending strong support in favor of the external shock model of GRBs. The width of the observed E_p distribution may be regarded as evidence for the existence of burst sources with a wide range of baryon loading factors Γ_0 , as suggested by Dermer et al. (1999a, 1999b). Our analysis only weakly constrains the existence of a population of dirty fireballs with lower values of Γ_0 , because these dirty fireballs are largely undetectable for BATSE due to the rapid decline of the observed peak flux in the BATSE photon energy range with decreasing Γ_0 . BATSE is therefore insensitive to a dirty fireball population except for the few events that occur at redshifts $z \ll 1$. The small number of GRBs with $E_p \lesssim 100$ keV in the data shown in Figs. 3, 4, and 5 might be, at least in part, an artifact of the selection bias mentioned at the beginning of the previous section, namely that E_p can only be determined for bright bursts, while dirty fireballs, producing spectra with low E_p , are intrinsically dim.

Also the existence of a population of clean fireball burst sources cannot be constrained tightly on the basis of our results. However, this conclusion is strongly dependent on the radiative regime of the average GRB blast wave. For the value $g = 1.7$ found in our study to be an appropriate choice to reproduce the peak flux, E_p and duration distributions, an additional population of clean fireballs with Γ_0 much larger than the upper limit quoted above ($\Gamma_0^{max} n_0^{1/8} \approx 462 \text{ cm}^{-3/8}$) can not be excluded, although it slightly worsens our modeling results. However, if a radiative regime $g \leq 1.6$ is assumed, the decline of the peak flux with increasing $\Gamma_0 > \bar{\Gamma}_0$ becomes much slower, implying that clean fireballs would be detected as high- E_p bursts, inconsistent with the observed E_p distribution.

We therefore conclude that our analysis is in accord with the existence of a class of dirty fireballs with $E_p \ll 100$ keV which have generally not been detected with BATSE. Also the existence of a significantly larger fraction of cleaner fireballs than detected by BATSE cannot be excluded from our analysis, although its consistency with observations depends strongly on the best-fit radiative regime of the average GRB blast wave.

Our results indicate that the most powerful GRBs can be detected at redshifts $z \gtrsim 4$. The

slope of $\sim 3/2$ in the peak flux distribution seems to be a coincidence due to the particular distribution of burst source energies, E_{52} , in combination with the non-Euclidean space-time geometry. This is in accord with the fact that the burst with the highest redshift measured so far, GRB 971214, still has a rather high BATSE peak flux and fluence, while the closest GRB for which a redshift estimate exists so far, GRB 980425, was a rather dim burst.

In summary, we use a parametrization of the blast wave model to calculate the peak flux, duration, and νF_ν peak energy of a GRB with a prescribed set of intrinsic and environmental parameters. We assume that the evolution of the GRB rate with redshift is proportional to the star-formation history of the universe. By taking into account triggering properties of GRB detectors in our calculations, we make a detailed comparison of model distributions with BATSE results for the peak flux, t_{50} , and E_p distributions. We have shown how these distributions can be self-consistently modeled and used to extract fireball model parameters. Our analysis shows that the observed statistical distributions of observables of GRBs are in accord with the scenario that GRBs are associated with sites of active star formation, although alternative cosmological distributions of GRB sources, which have not been considered in this paper, cannot be excluded. Future work must consider evolutionary behaviors to test compact object coalescence scenarios. We argue that the short, hard GRBs represent a separate population of burst sources.

We thank the anonymous referee for very helpful comments which led to considerable improvements of the manuscript. We also thank J. Chiang for useful comments. This work is partially supported by NASA grant NAG 5-4055. CD acknowledges support from the Office of Naval Research.

REFERENCES

- Band, D., Matteson, J., Ford, L., et al., 1993, ApJ, 413, 281
- Bloom, J. S., Djorgovski, S. G., Kulkarni, S. R., & Frail, D. A. 1998a, ApJ, 507, L105
- Bloom, J. S., et al. 1998b, ApJ, 508, L21
- Bloom, J. S., et al., 1999, ApJL, submitted
- Chiang, J., & Dermer, C. D., 1999, ApJ, 512, 699
- Costa, E., et al. 1997, Nature, 387, 783
- Crider, A. W., Liang, E. P., Smith, I. A., et al., 1997, ApJ, 479, L39
- Dermer, C. D., Chiang, J., & Böttcher, M., 1999a, ApJ, 513, 656
- Dermer, C. D., Böttcher, M., & Chiang, J., 1999b, ApJL, 515, L49

- Dermer, C. D., & Mitman, K. E., 1999, *ApJ*, 513, L5
- Djorgovski, S. G., Kulkarni, S. R., Bloom, J. S., Goodrich, R., Frail, D. A., Piro, L., & Palazzi, E., 1998, *ApJ*, 508, L17
- Djorgovski, S. G., Kulkarni, S. R., Bloom, & Frail, D. A. 1999a, GCN 289
- Djorgovski, S. G., 1999, report at Santa Barbara Institute for Theoretical Physics Workshop on Gamma Ray Bursts
- Djorgovski, S. G., et al., 1999b, GCN Circ. 189
- Eichler, D., Livio, M., Piran, T., & Schramm, D. N. 1989, *Nature*, 340, 126
- Fenimore, E. E., Epstein, R. I., Ho, C., et al., 1993, *Nature*, 366, 40
- Fenimore, E. E., & Bloom, J. S., 1995, *ApJ*, 453, 25
- Fishman, G. J., & Meegan, C. A., 1995, *ARAA*, 33, 415
- Fishman, G. J., et al. 1994, *ApJS*, 92, 229
- Frail, D. 1998, in the Fourth Huntsville Gamma-Ray Burst Symposium, ed. C. A. Meegan, R. D. Preece, & T. M. Koshut (AIP: New York), 563
- Galama, T. J., et al. 1998, *Nature*, 395, 670
- Katz, J. I., & Canel, L. M., 1996, *ApJ*, 471, 915
- Kelson, D. D., Illingworth, G. I., Franx, M., Magee, D., & van Dokkum, P. G., 1999, *IAU Circ.* 7096
- Kommers, J. M., Lewin, W. H. G., Kouveliotou, C., et al., 1998, *ApJ*, submitted (astro-ph/9809300)
- Kouveliotou, C., et al., 1993, *ApJ*, 413, L101
- Krumholz, M., Thorsett, S. E., & Harrison, F. A., 1998, *ApJ*, 506, L81
- Kulkarni, S., presentation at “Gamma-Ray Bursts in the Afterglow Era,” 3-6 November, 1998, Rome, Italy
- Kulkarni, S., et al., 1998a, *Nature*, 395, 663
- Kulkarni, S., et al., 1998b, *Nature*, 393, 35
- Lilly, S. J., LeFèvre, O., Hammer, F., & Crampton, D., 1996, *ApJ*, 460, L1
- Madau, P., Ferguson, H. C., Dickinson, M. E., et al., 1996, *MNRAS*, 283, 1388
- Madau, P., Pozzetti, L., & Dickinson, M., 1998, *ApJ*, 498, 106

- Mallozzi, R. S., Paciesas, W. S., Pendleton, G. N., et al., 1995, *ApJ*, 454, 597
- Mallozzi, R. S., Pendleton, G. N., & Paciesas, W. S., 1996, *ApJ*, 471, 636
- Mallozzi, R. S., Pendleton, G. N., Paciesas, W. S., et al., 1997, in 4th Huntsville Symposium on Gamma-Ray Bursts, eds. Meegan, C. A., Preece, R. D., & Koshut, T. M., p. 273
- Meegan, C. A., Pendleton, G. N., Briggs, M. S., et al., 1996, *ApJS*, 106, 65
- Meegan, C. A., Paciesas, W. S., Pendleton, G. N., et al., 1997, in 4th Huntsville Symposium on Gamma-Ray Bursts, eds. Meegan, C. A., Preece, R. D., & Koshut, T. M., p. 3
- Metzger, M. R., Djorgovski, S. G., Kulkarni, S. R., et al., 1998, *Nature*, 387, 878
- Mitrofanov, I. G., et al., 1993, in 2nd Compton Symposium, ed. M. Friedlander, N. Gehrels, & D. J. Macomb (New York: AIP Conf. Proc. 280), 761
- Narayan, R., Paczyński, B., & Piran, T. 1992, *ApJ*, 395, L83
- Norris, J. P., Nemiroff, R. J., Scargle, J. D., et al., 1994, *ApJ*, 424, 540
- Paczyński, B., 1998, *ApJ*, 494, L45
- Perna, R., Raymond, J., & Loeb, A., 1999, *ApJ*, submitted (astro-ph/9904181)
- Piro, L., et al., 1999, *ApJ*, 514, L73
- Preece, R. D., Pendleton, G. N., Briggs, M. S., Mallozzi, R. S., Paciesas, W. S., Band, D. L., Matteson, J. L., & Meegan, c. A., 1998a, *ApJ*, 496, 849
- Preece, R. D., Briggs, M. S., Mallozzi, R. S., et al., 1998b, *ApJ*, 506, L23
- Rees, M. J., & Mészáros, P. 1992, *MNRAS*, 258, 41P
- Strohmayer, T. E., Fenimore, E. E., Murakami, T., & Yoshida, A. 1998, *ApJ*, 500, 873
- Tavani, M., 1998, *ApJ*, 497, L21
- Totani, T., 1997, *ApJ*, 486, L71
- Totani, T., Yoshii, Y., & Sato, K., 1997, *ApJ*, 483, L75
- Totani, T., 1999, *ApJ*, 511, 41
- van Paradijs, J., et al. 1997, *Nature*, 386, 686
- Vietri, M., & Stella, L., 1998, *ApJ*, 507, L45
- Waxman, E. 1997, *ApJ*, 489, L33

Wijers, R. A. M. J., et al., 1998, MNRAS, 294, L13

Woosley, S. E. 1993, ApJ, 405, 273

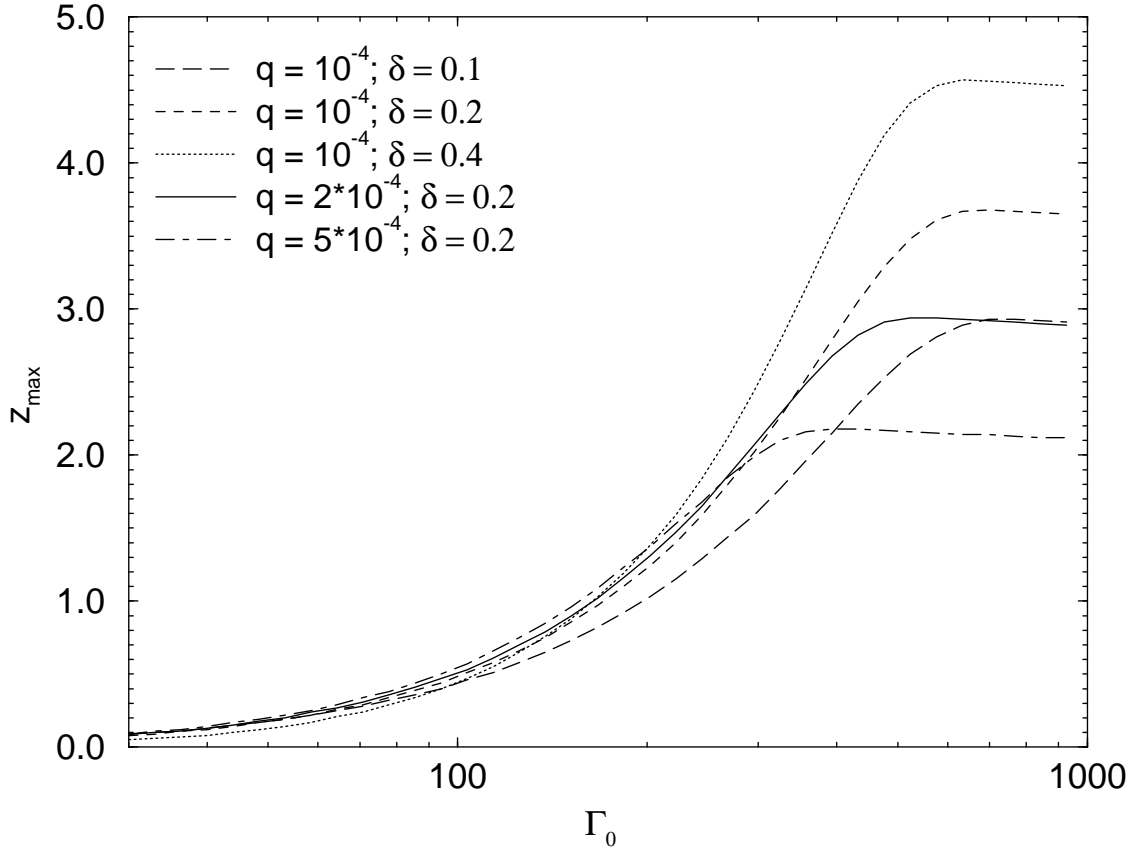


Fig. 1.— The maximum redshift out to which a GRB can be detected above the 1024 ms trigger threshold $\Phi_{lim} \approx 0.2$ photons $\text{cm}^{-2} \text{s}^{-1}$, as a function of baryon loading factor Γ_0 , equipartition factor q , and high-energy νF_ν spectral index δ . Parameters: $E_0 = 10^{53}$ erg, $n_0 = 100 \text{ cm}^{-3}$, $g = 1.6$.

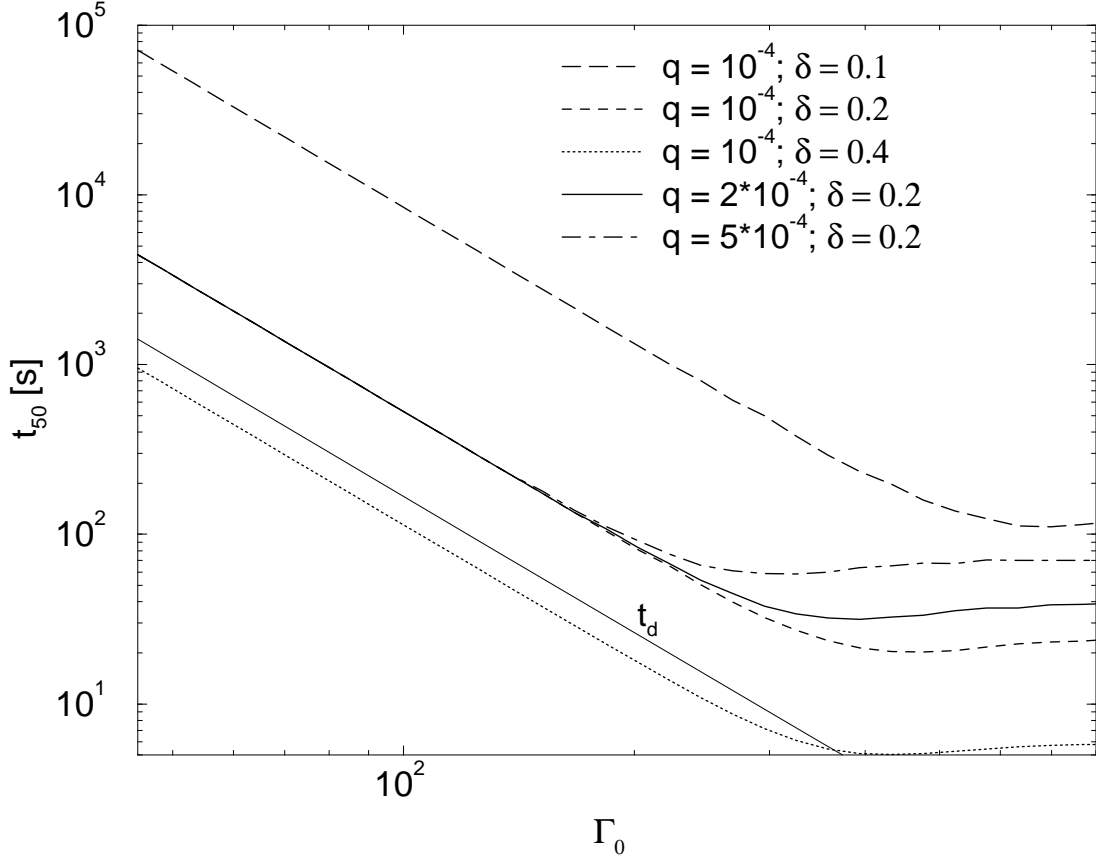


Fig. 2.— Burst duration t_{50} for a standard GRB located at $z = 1$, as a function of Γ_0 , q , and δ . Other parameters: $E_0 = 10^{53}$ erg, $n_0 = 100 \text{ cm}^{-3}$, $g = 1.6$. The light solid curve shows the deceleration time t_d for comparison.

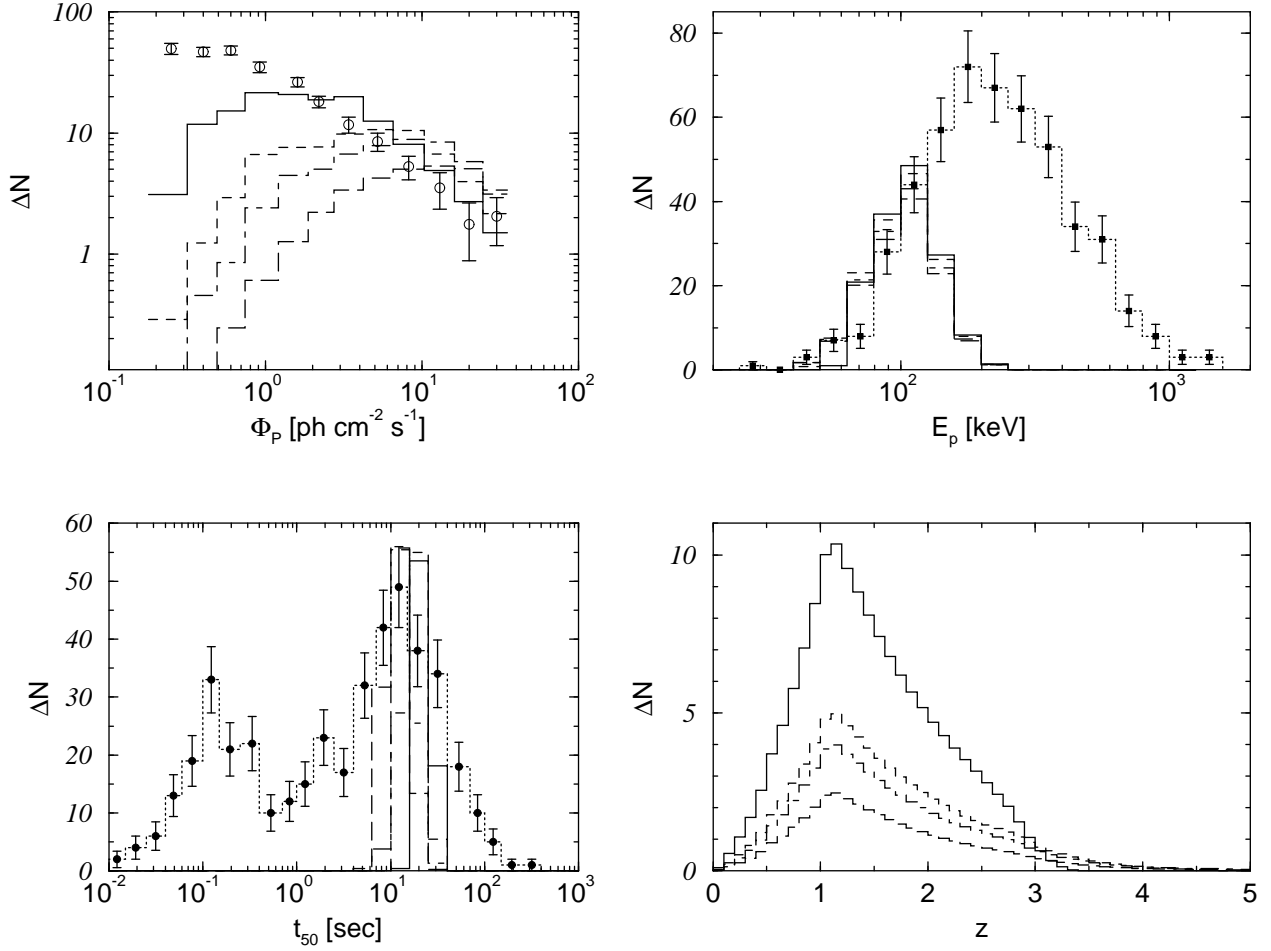


Fig. 3.— Comparison of peak flux, E_{pk} , t_{50} and redshift distributions for a set of burst parameters $E_{52} = 50$, $\Gamma_0 = 240$, $n_0 = 100 \text{ cm}^{-3}$, $q = 5 \cdot 10^{-4}$, for different radiative regimes of the blast wave, i. e. different values of g : $g = 1.6$ (solid histograms); $g = 1.8$ (dashed histograms); $g = 2.1$ (dot-dashed histograms); $g = 2.8$ (long-dashed histograms).

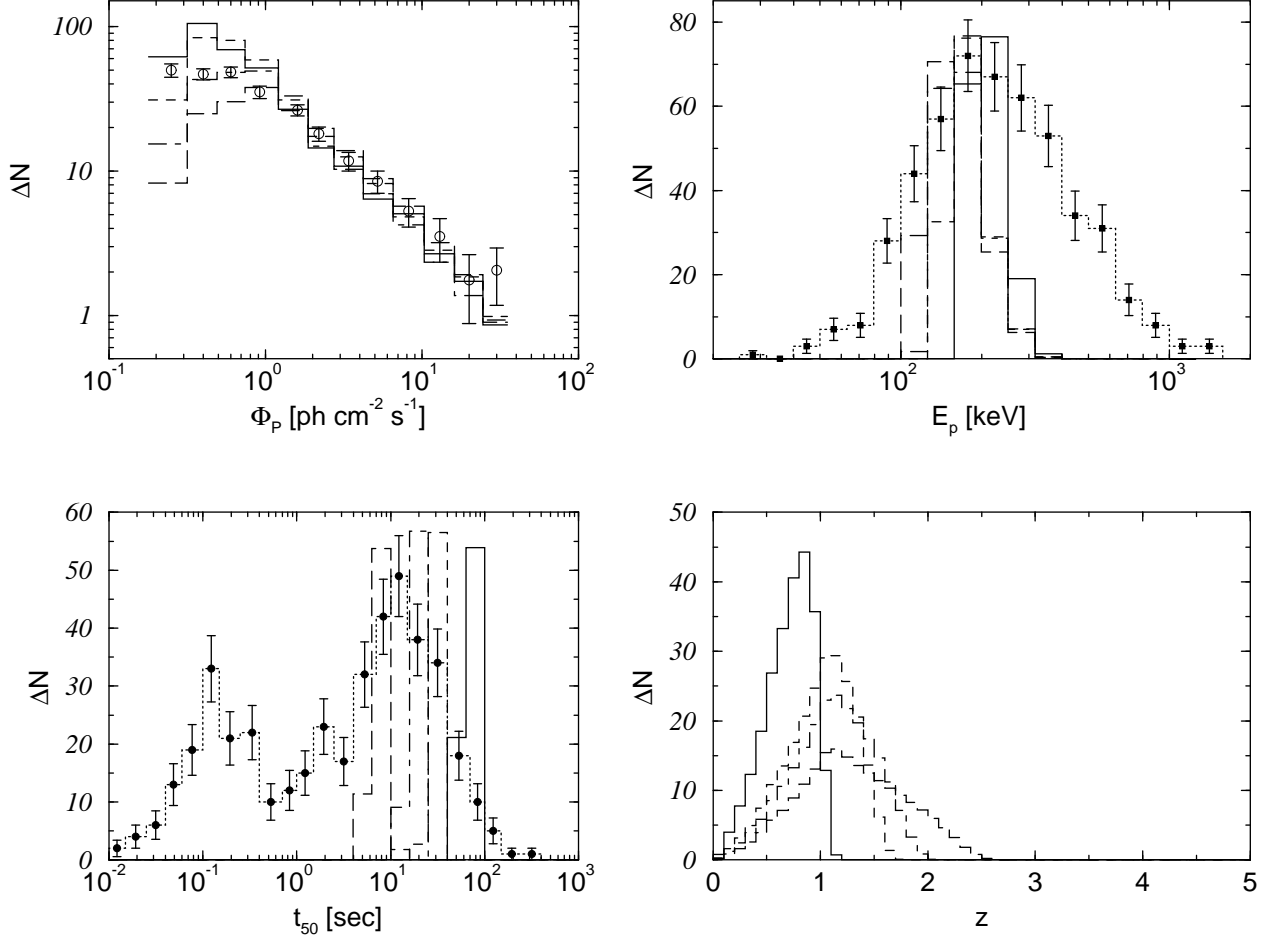


Fig. 4.— Comparison of peak flux, E_{pk} , t_{50} and redshift distributions for a set of burst parameters $E_{52} = 3.8$, $\Gamma_0 = 220$, $n_0 = 100 \text{ cm}^{-3}$, $q = 10^{-3}$, $\delta = 0.2$, for different values of g : $g = 1.6$ (solid histograms); $g = 1.8$ (dashed histograms); $g = 2.1$ (dot-dashed histograms); $g = 2.8$ (long-dashed histograms).

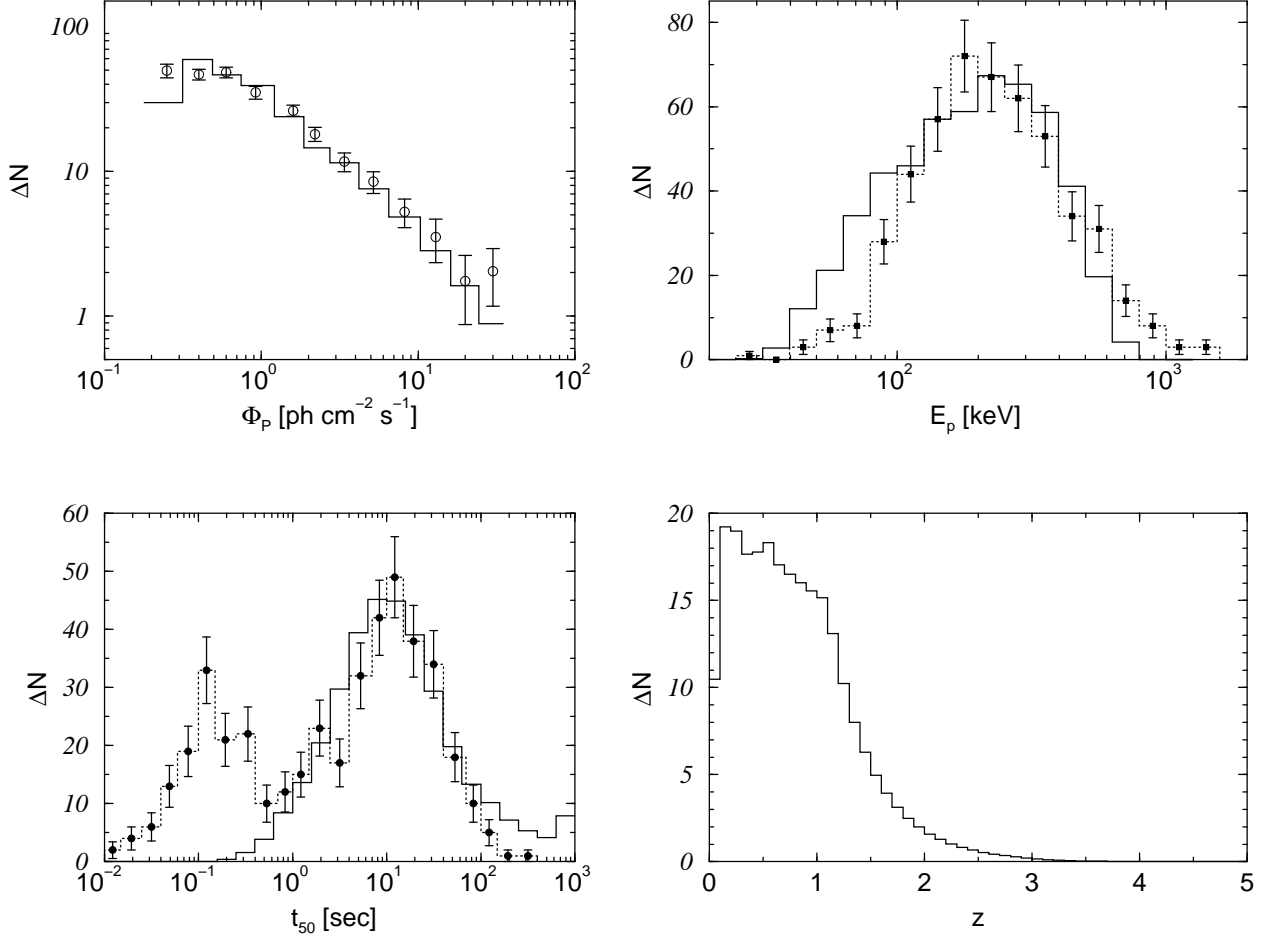


Fig. 5.— Comparison of our model burst population to the 3B catalog peak flux, E_{pk} , and t_{50} distributions, and model redshift distribution. Parameters: $10^{-4} \leq E_{52} \leq 100$, $e = 1.52$, $\Gamma_0 \leq 260$, $\gamma = 0.25$, $n_0 = 100 \text{ cm}^{-3}$, $g = 1.7$, $q = 10^{-3}$.

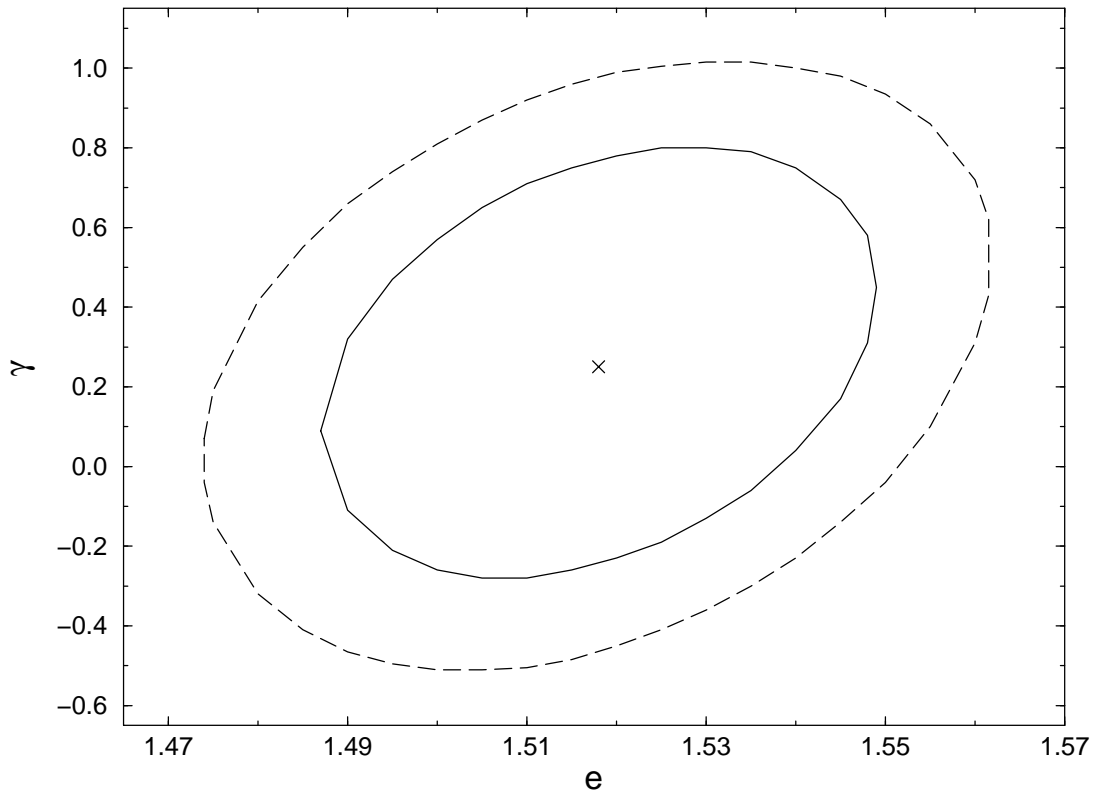


Fig. 6.— 1σ (solid line) and 2σ (dashed line) confidence contours of the parameters e and γ parametrizing the distributions of total blast wave energy and baryon loading factor, respectively ($N(E_{52}) \propto E_{52}^{-e}$, $N(\Gamma_0) \propto \Gamma_0^{-\gamma}$), for a standard set of values: $g = 1.7$, $q = 10^{-3}$, $\Gamma_{0,\max} = 260$, $n_0 = 100 \text{ cm}^{-3}$.